ROCKET THERMAL ANALYSIS		
	Tau Rocket Team	
	Project Phase: PDR	Subsystem: Propulsion
	Responsible: Andres Benoit	Project: LASC Cooperation
Authors: João Vítor Bernardi Rohr, Andres Gilberto Machado da Silva Benoit		

Abstract

For decades rocket groups have been using the THERMCAS software as a mean of initial estimations for the thermal analysis of a Solid Rocket Motor. Aiming to provide a better and more intuitive software, a new software was developed, Rocket Thermal Analysis (RTA). By applying the Finite Difference Method in analytical equations for convection and conduction, models for the casing and bulkhead heat distribution were successfully implemented inside RTA. The outputs showed good accordance with the expected values and the software is available for download on our Github repository.

Contents

1 Software Purpose

The idea of developing RTA was brought to light by the Propulsion subsystem at the Latin America Space Challenge Cooperation 2021, during 2020. It was proposed a new software to replace the old THERMCAS [4], created by Richard Nakka. During the RTA development it was always in our mind that the software needed to be easy to execute and run a simulation and should have more features than THERMCAS does. This is why in RTA a bulkhead analysis is able to be conducted as well as two Finite Difference Methods for the casing thermal distribution. It is planned the insertion of many material properties for the user to choose, since now only EPDM and Aluminium 6061-T6 are available.

2 Software Explanation

2.1 Casing

For a thin cylinder of lenght to radius ratio of about 10, an infinite cylinder having only one dimension for conduction can be assume as an approximation [1], since the only considerable heat conduction path is radially. Solid Rocket Motors usually have a lenght to diameter ratio of 10 [2], so it is suitable to apply such an idealization in these applications.

Inside the rocket chamber the insulator area most exposed to hot gases are in the sections between grains. These areas will be receiving heat for a longer time than any other along the casing and by having so it is the critical point for heat insulation. Having said that, the heat exposure time will be set as the combustion time and an even thickness will be assumed throughout the insulator.

At first, heat will enter the system through convection by the hot gases provenient from the propellant burning. In order to have an estimation of the convective heat coefficent, an expression for convection in tube with turbulent flow can be used [1], it is shown in the Annex I. The convective heat will then be calculated utilizing Newton's Law of Cooling, considering the chamber and wall temperature.

After that, the boundary condition is set by applying the Energy Balance Equation at the first node, all the expressions are present in Annex I. The heats entering are from conduction from the posterior node and convection by the gases.

Then, conduction is taken within the materials. For that, a one-dimensional transient Fourier Law is applied, giving the care to change between the properties of the insulator and the casing structural material. The initial temperature of the materials composing the wall are set as the ambient temperature through all of its extent.

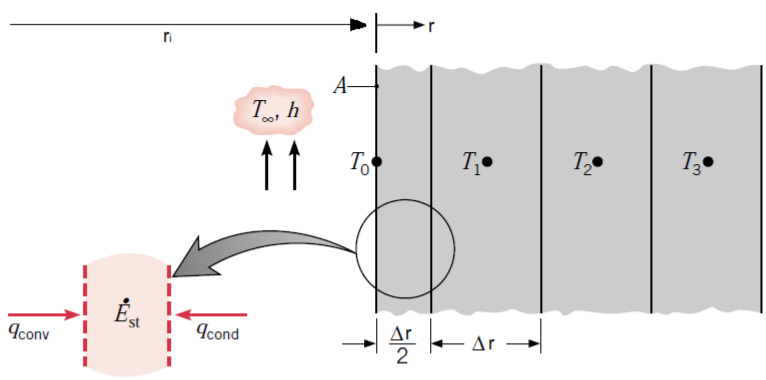

Figure 1: Discretization of the 1-D model. Adapted from [1].

2.2 Bulkhead

In order to tackle the bulkhead temperature distribution a two-dimensional model was addopted, it was based on cylindrical coordinates assuming symmetry along the angular coordinate. The bulkhead is considered here as a cylinder that is receiving heat on one of its circular surfaces. At the bulkhead side that is within the chamber an insulator of radius equal to that of the chamber is adopted.

The same equations used for the casing convective heat were used for the bulkhead scheme now for all the first line of nodes, see Annex II. For conduction the equations were used in two dimensions, going radially from Δr to the outer radius and in height from zero to the bulkhead thickness, see Annex II.

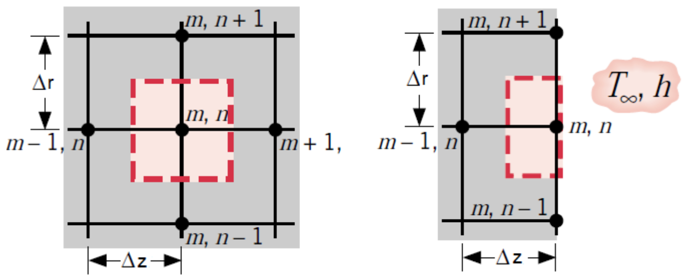

Figure 2: Discretization of the 2-D model. Adapted from [1].

2.3 Solution Methods

The method chosen to solve the partial differential equations was the Finite Difference Method because of its simplicity and fairly good results. For the casing an explicit and implicit form of the method was developed, but for the bulkhead only the explicit version was succesfully implemented. The reason for this is that to solve the equation implicitly it was required to solve simultaneously for nodes varying in r and z, which could not be done by the ease it was done in the one-dimension scheme.

In the Explicit Finite Difference Method the future temperature of a node was only dependent on previously known temperatures in its surroundings [1], so it was possible to program the code to solve the temperature for each node at a given time, see Annex I and II. This process is computationally costly and is able to not converge which is a downside. But it can achieve the objective once one is capable of accepting these faults.

In the other hand the Implicit Finite Difference Method created a system of algebraic equations that gave the previous temperature at the node based on the future temperature of the node and its surroundings [1], see Annex I. In order to solve this system the inverse matrix of the coefficients multiplying the new temperatures was calculated and then multiplied with the known temperatures vector to achieve the new temperature vector.

2.4 Graphical Resources

The RTA software has three options of graphs to be generate, those are:

Casing Temperature Distribution: a graph showing the temperature at each location of the casing wall at the end time.

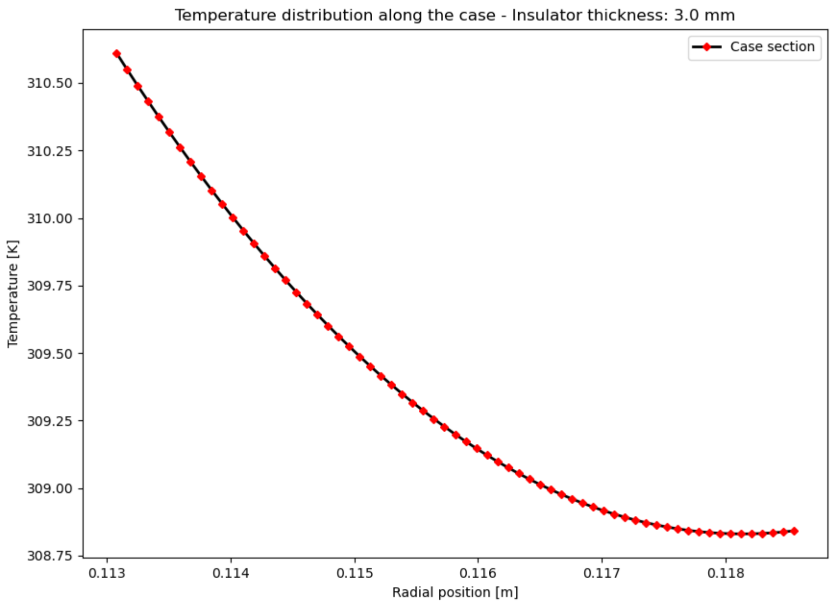

Figure 3: Graph of the casing temperature distribution.

Casing and Insulator Temperature Distribution: it is generated a graph showing the temperature distribution across all of the spatial domain at the end time.

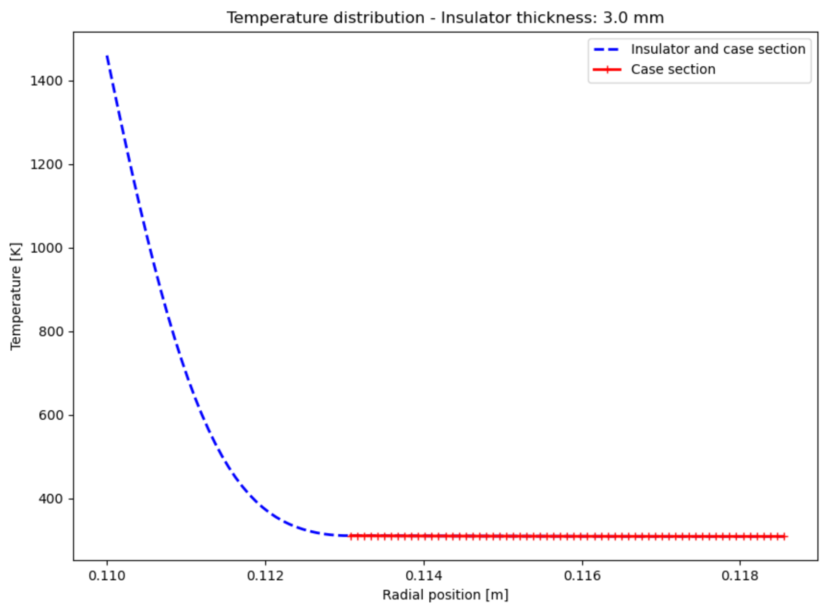

Figure 4: Graph of the casing and insulator temperature distribution.

Temperature Distribution at different times: the plot will show the temperature distribution at the last node for times going from 0 to 100% of the total burn time, with a pace of 25%.

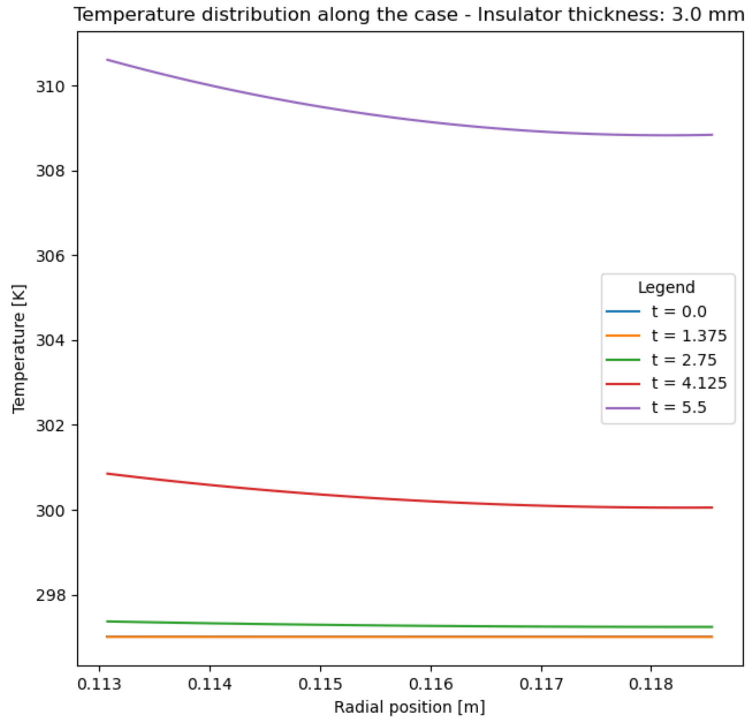

Figure 5: Temperature Distribution at different times.

2.5 Output File

RTA provides an optional output text file in which it provides in details the principal inputs for the analysis and of course a data frame which contains the results, but there are several differences between the output file of the implicit and of the explicit method and also with respect to bulkhead resultant file, the differences are shown below.

2.5.1 Case output file for implicit method

- It has detailed information about the inputs;
- It displays a dataframe with the results;
- If time or radial steps exceed 1000 it will generate a resumed file.

It is possible to see a typical output file below

```
Output file generated by Rocket Thermal Analysis

Type of analysis: Case temperature distribution

Analysis Information:
 Case material: Aluminum 6061 - T6
 Insulator Material: EPDM
 Insulator thickness: 0.003 m
 Case thickness: 0.00555 m
 Inner cylinder radius: 0.11 m
 Time Steps: 250
 Burn time: 5 s
 Radial Steps: 16
 Convection coefficient: 1295 W/m2-K
 Initial case temperature: 298 K
 Combustion Temperature: 1600 K

Date:2020-10-23 22:40:20.612627

Method:Implicit

The following dataframe is organized by Time step x Radial position
```

	0	1	2	3	4	5	6	7	8	9	10	11	12	13	14	15	16
0	371.378050	298.000000	298.000000	298.000000	298.000000	298.000000	298.000000	298.000000	298.000000	298.000000	298.000000	298.000000	298.000000	298.000000	298.000000	298.000000	298.000000
1	439.519642	298.577304	298.004615	298.000037	298.000000	298.000000	298.000000	298.000000	298.000000	298.000000	298.000000	298.000000	298.000000	298.000000	298.000000	298.000000	298.000000
2	502.807058	299.681606	298.017986	298.000180	298.000002	298.000000	298.000000	298.000000	298.000000	298.000000	298.000000	298.000000	298.000000	298.000000	298.000000	298.000000	298.000000
3	561.594551	301.266440	298.043815	298.000528	298.000006	298.000000	298.000000	298.000000	298.000000	298.000000	298.000000	298.000000	298.000000	298.000000	298.000000	298.000000	298.000000
4	616.210400	303.288890	298.085403	298.001202	298.000015	298.000000	298.000000	298.000000	298.000000	298.000000	298.000000	298.000000	298.000000	298.000000	298.000000	298.000000	298.000000
5	666.958821	305.709330	298.145683	298.002348	298.000034	298.000000	298.000000	298.000000	298.000000	298.000000	298.000000	298.000000	298.000000	298.000000	298.000000	298.000000	298.000000
6	714.121730	308.491176	298.227250	298.004127	298.000066	298.000001	298.000001	298.000001	298.000000	298.000000	298.000000	298.000000	298.000000	298.000000	298.000000	298.000000	298.000000
7	757.960381	311.600665	298.332389	298.006719	298.000119	298.000002	298.000001	298.000001	298.000001	298.000001	298.000000	298.000000	298.000000	298.000000	298.000000	298.000000	298.000000
8	798.716881	315.006640	298.463099	298.010315	298.000200	298.000004	298.000003	298.000002	298.000001	298.000001	298.000001	298.000001	298.000000	298.000000	298.000000	298.000000	298.000000
9	836.615598	318.680358	298.621122	298.015118	298.000317	298.000006	298.000004	298.000003	298.000002	298.000002	298.000001	298.000001	298.000001	298.000001	298.000001	298.000000	298.000000
10	871.864459	322.595311	298.807959	298.021339	298.000483	298.000010	298.000007	298.000006	298.000004	298.000003	298.000002	298.000002	298.000001	298.000001	298.000001	298.000001	298.000001
11	904.656158	326.727060	299.024895	298.029196	298.000709	298.000015	298.000012	298.000009	298.000007	298.000005	298.000004	298.000003	298.000002	298.000002	298.000002	298.000002	298.000002
12	935.169276	331.053076	299.273016	298.038913	298.001009	298.000023	298.000018	298.000014	298.000010	298.000008	298.000006	298.000005	298.000004	298.000003	298.000003	298.000003	298.000003
13	963.569315	335.552603	299.553224	298.050717	298.001398	298.000034	298.000027	298.000020	298.000016	298.000012	298.000009	298.000007	298.000006	298.000005	298.000004	298.000004	298.000004
14	990.009654	340.206522	299.866260	298.064839	298.001895	298.000049	298.000038	298.000030	298.000023	298.000018	298.000014	298.000011	298.000009	298.000008	298.000007	298.000006	298.000006
15	1014.632447	344.997230	300.212711	298.081509	298.002516	298.000069	298.000054	298.000042	298.000033	298.000026	298.000020	298.000016	298.000013	298.000011	298.000010	298.000009	298.000009
16	1037.569437	349.908524	300.593027	298.100959	298.003284	298.000095	298.000075	298.000059	298.000046	298.000036	298.000029	298.000023	298.000019	298.000016	298.000015	298.000014	298.000014
17	1058.942728	354.925500	301.007536	298.123418	298.004219	298.000128	298.000101	298.000080	298.000063	298.000050	298.000040	298.000033	298.000027	298.000023	298.000021	298.000020	298.000020
18	1078.865486	360.034452	301.456449	298.149115	298.005345	298.000170	298.000135	298.000107	298.000086	298.000069	298.000055	298.000045	298.000038	298.000033	298.000029	298.000028	298.000028
19	1097.442599	365.222783	301.939879	298.178275	298.006686	298.000222	298.000177	298.000142	298.000114	298.000092	298.000075	298.000061	298.000052	298.000045	298.000040	298.000038	298.000038
20	1114.771280	370.478923	302.457843	298.211122	298.008269	298.000286	298.000230	298.000185	298.000149	298.000121	298.000099	298.000082	298.000069	298.000060	298.000055	298.000052	298.000052
21	1130.941635	375.792249	303.010277	298.247873	298.010121	298.000365	298.000295	298.000239	298.000193	298.000158	298.000130	298.000108	298.000092	298.000080	298.000073	298.000069	298.000070
22	1146.037180	381.153015	303.597041	298.288744	298.012271	298.000460	298.000374	298.000304	298.000247	298.000203	298.000168	298.000140	298.000120	298.000105	298.000096	298.000092	298.000092
23	1160.135327	386.552284	304.217927	298.333943	298.014748	298.000574	298.000468	298.000383	298.000313	298.000258	298.000214	298.000180	298.000155	298.000137	298.000125	298.000120	298.000120
24	1173.307831	391.981871	304.872666	298.383674	298.017585	298.000710	298.000582	298.000477	298.000393	298.000325	298.000271	298.000229	298.000198	298.000175	298.000161	298.000154	298.000155
25	1185.621202	397.434280	305.560937	298.438137	298.020813	298.000871	298.000716	298.000590	298.000488	298.000405	298.000340	298.000289	298.000250	298.000223	298.000205	298.000197	298.000197
26	1197.137095	402.902656	306.282370	298.497523	298.024465	298.001060	298.000875	298.000724	298.000600	298.000501	298.000422	298.000360	298.000314	298.000280	298.000259	298.000249	298.000249
27	1207.912661	408.380734	307.036552	298.562020	298.028576	298.001280	298.001060	298.000880	298.000733	298.000615	298.000520	298.000446	298.000390	298.000349	298.000324	298.000311	298.000312
28	1218.000881	413.862797	307.823032	298.631807	298.033182	298.001535	298.001276	298.001063	298.000889	298.000748	298.000636	298.000547	298.000480	298.000432	298.000401	298.000387	298.000387
29	1227.450868	419.343627	308.641326	298.707059	298.038317	298.001829	298.001526	298.001276	298.001071	298.000905	298.000771	298.000667	298.000587	298.000530	298.000493	298.000476	298.000477
30	1236.308154	424.818477	309.490922	298.787943	298.044020	298.002166	298.001813	298.001522	298.001282	298.001087	298.000930	298.000807	298.000713	298.000646	298.000602	298.000582	298.000583
31	1244.614951	430.283024	310.371283	298.874619	298.050327	298.002551	298.002142	298.001804	298.001525	298.001297	298.001114	298.000970	298.000860	298.000781	298.000730	298.000706	298.000708
32	1252.410394	435.733345	311.281850	298.967241	298.057277	298.002988	298.002517	298.002126	298.001803	298.001539	298.001327	298.001159	298.001031	298.000939	298.000879	298.000851	298.000853
33	1259.730765	441.165881	312.222045	299.065956	298.064908	298.003483	298.002943	298.002493	298.002121	298.001817	298.001571	298.001377	298.001228	298.001121	298.001053	298.001020	298.001022
34	1266.609706	446.577411	313.191275	299.170904	298.073261	298.004040	298.003424	298.002909	298.002483	298.002133	298.001850	298.001627	298.001456	298.001332	298.001253	298.001215	298.001218
35	1273.078410	451.965025	314.188935	299.282219	298.082375	298.004666	298.003965	298.003379	298.002892	298.002493	298.002169	298.001912	298.001716	298.001574	298.001483	298.001440	298.001443
36	1279.165799	457.326099	315.214410	299.400028	298.092290	298.005366	298.004572	298.003907	298.003354	298.002899	298.002530	298.002237	298.002013	298.001851	298.001746	298.001697	298.001701
37	1284.898694	462.658273	316.267076	299.524450	298.103048	298.006146	298.005250	298.004499	298.003873	298.003357	298.002938	298.002605	298.002350	298.002165	298.002047	298.001990	298.001995
38	1290.301965	467.959432	317.346303	299.655599	298.114688	298.007012	298.006005	298.005159	298.004454	298.003871	298.003397	298.003021	298.002731	298.002522	298.002387	298.002324	298.002329
39	1295.398677	473.227684	318.451457	299.793583	298.127252	298.007972	298.006844	298.005895	298.005102	298.004447	298.003913	298.003488	298.003161	298.002925	298.002773	298.002701	298.002707
40	1300.210219	478.461343	319.581901	299.938501	298.140783	298.009032	298.007773	298.006712	298.005823	298.005088	298.004489	298.004011	298.003644	298.003378	298.003207	298.003126	298.003133
41	1304.756432	483.658916	320.737000	300.090447	298.155320	298.010200	298.008798	298.007615	298.006624	298.005802	298.005131	298.004596	298.004184	298.003886	298.003694	298.003603	298.003611
42	1309.055714	488.819080	321.916114	300.249509	298.170907	298.011482	298.009927	298.008612	298.007509	298.006593	298.005845	298.005248	298.004788	298.004454	298.004239	298.004138	298.004147
43	1313.125134	493.940675	323.118610	300.415769	298.187584	298.012888	298.011166	298.009709	298.008485	298.007468	298.006636	298.005971	298.005458	298.005087	298.004847	298.004734	298.004745
44	1316.980524	499.022691	324.343854	300.589302	298.205393	298.014424	298.012524	298.010913	298.009559	298.008432	298.007510	298.006772	298.006203	298.005790	298.005523	298.005398	298.005410
45	1320.636572	504.064249	325.591218	300.770179	298.224376	298.016099	298.014008	298.012232	298.010737	298.009493	298.008473	298.007656	298.007026	298.006568	298.006273	298.006135	298.006149
46	1324.106903	509.064598	326.860076	300.958463	298.244576	298.017922	298.015625	298.013673	298.012028	298.010656	298.009531	298.008630	298.007934	298.007428	298.007103	298.006950	298.006965

Figure 6: Typical implicit method output file.

2.5.2 Case output file for explicit method

- It has detailed information about the inputs;
- It displays a dataframe with the results;
- The dataframe contains 10 values for time steps represeting a percentage of the burning time.

It is possible to see a typical output file below

```
Output file generated by Rocket Thermal Analysis

Type of analysis: Case temperature distribution

Analysis Information:
 Case material: Aluminum 6061 - T6
 Insulator Material: EPDM
 Insulator thickness: 0.003 m
 Case thickness: 0.00555 m
 Inner cylinder radius: 0.11 m
 Time Steps: 3200
 Burn time: 5 s
 Radial Steps: 16
 Convection coefficient: 1295 W/m2-K
 Initial case temperature: 298 K
 Combustion Temperature: 1600 K

Date:2020-10-23 22:41:10.190627

Method:Explicit

The following dataframe is organized by Time step x Radial position
```

	0	1	2	3	4	5	6	7
0%	298.000000	298.000000	298.000000	298.000000	298.000000	298.000000	298.000000	298.000000
10%	767.615265	343.796094	301.025266	298.150583	298.006001	298.000204	298.000163	298.000130
20%	1027.564572	433.628280	315.516632	299.724610	298.136887	298.009522	298.008256	298.007182
30%	1177.022144	529.517361	341.515490	304.312754	298.743593	298.078975	298.071189	298.064449
40%	1266.851975	617.586996	375.323920	312.633031	300.266802	298.325441	298.300473	298.278637
50%	1323.581406	694.059050	413.229421	324.587584	303.067301	298.918765	298.862246	298.812529
60%	1361.321615	759.089550	452.472209	339.619424	307.353950	300.049493	299.946231	299.855082
70%	1387.754819	814.135976	491.268806	357.007777	313.186292	301.897096	301.733665	301.589112
80%	1407.176543	860.891379	528.583953	376.044671	320.510443	304.608097	304.374478	304.167615
90%	1422.062340	900.897002	563.889910	396.118392	329.201014	308.285489	307.975733	307.701338
100%	1433.853955	935.336234	596.878737	416.674872	339.063852	312.970822	312.583231	312.239915

Figure 7: Typical explicit method output file.

2.5.3 Bulkhead output file

Unfortunately for this first release it will be unavailable to generate an output file for the bulkhead.

3 Stability Analysis

Solving a Partial Differential Equation by the Finite Difference Method and utilizing an Explicit approach requires a stability criterion to be respected for the solution to converge. This criterion, for a parabollic PDE, is, according to the Von Neumann necessary condition for stability, that the coefficient of the associated node of interest at the previous time is greater than or equal to zero [3].

For the 1-D solution, applied to the casing model, this condition gives the following relation between the finite step in time and the finite step in space.

$$\Delta t \leq \frac{(\Delta r)^2}{2\alpha} \tag{1}$$

It happens to be that the above expression is equivalent to the criterion of having a fourier number smaller than 0.5, so when the user is putting the data in RTA, the software will ask for you to get down its value until the Fourier Number reaches a number below 0.5. The same criteria was analyses for the 2-D solution of the bulkhead model. In that case, the expression is

$$\Delta t \leq \frac{(\Delta z \Delta r)^2}{2\alpha(\Delta r^2 + \Delta z^2)} \tag{2}$$

An exemple of how the solution behaves when the time and spatial steps are changed can be seen in Figure 1. Fixing the number of time steps in $n_t = 120$ in the right hand side and fixig the spatial steps in $n_r = 120$ for the left hand side.

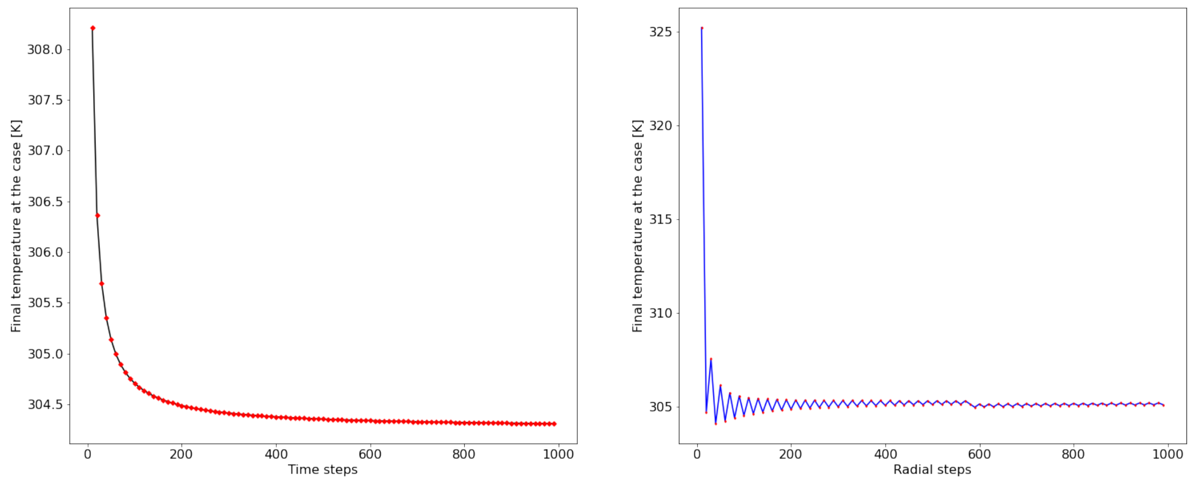

Figure 8: Convergence of the solution varying time and space steps.

As can be seen in the Figure 8, for 200 time steps the solution already has a good precision, being it deviated by 0.1 from the limit result at that point. For the amplitude of the radial steps temperature oscillation to remain approximately constant it is required about 300 steps, the result will be approximately 0.5 Kelvin deviated from the limit result.

4 Results Comparison

In order to have a comparison between the explicit, implicit and THERMCAS outputs, a simulation was conducted in the three of them, all with the same values. Because THERMCAS has a limit of 10 radial points, the same amount was used in the RTA. The values used are listed in the table below.

Variable	Description	Insulator	Casing
C_p	Specific Heat $[J/kgK]$	2000	896
ρ	Specific Mass $[kg/m^3]$	860	2700
k	Thermal Conductivity $[W/mK]$	0.2	167
tk_0	Casing thickness $[mm]$	5.55	
tk_0	Insulator thickness $[mm]$	3	
r_i	Inner radius $[m]$	0.11	
t	Burn time $[s]$	5	
n_t	Number of time steps	250	
n_r	Number of radial points	10	
Δr	Radial step $[mm]$	0.555	
Δt	Time step $[s]$	0.02	
h_m	Convection Coefficient $[W/m^2K]$	1295	
T_i	Initial Temperature $[K]$	297	
T_c	Combustion Temperature $[K]$	1600	

Table 1: Values used in the simulations.

From the simulation run, the plots shown below were obtained. In it, one can identify the clear difference between THERMCAS and RTA, both explicit and implicit methods showed good accordance, but in the other way, THERMCAS got smaller and constant values.

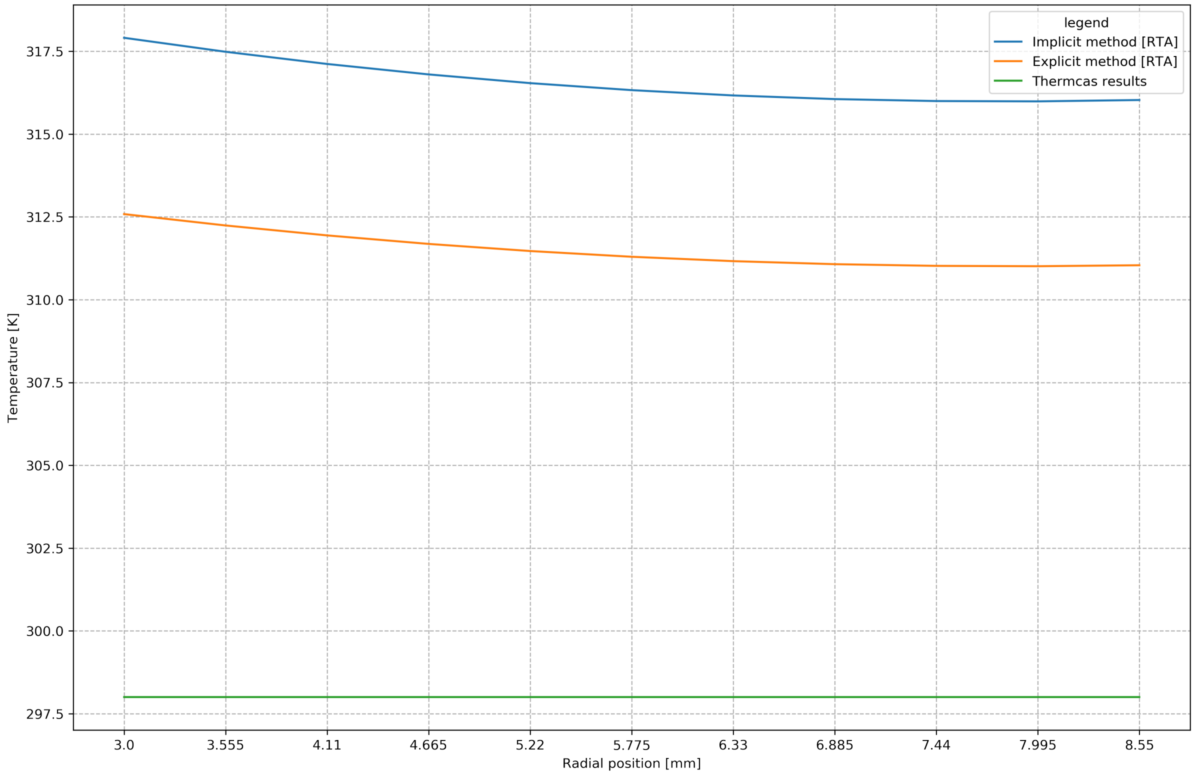

Figure 9: Casing temperature distribution after 5 seconds.

In THERMCAS, the outputs are rounded, so for the first point of the casing to the last temperature did not change one degree Celsius. This seems unreasonable for the inputs provided.

These clearly different results came from the fact that the two approches to the problem are different. THERMCAS considers the coordinate as cartesian, an evidence is that the software does not ask for the radius of the combustion chamber, so its model is an infinite plane. In the other way, at RTA the coordinate system is cylindrical, so the model is an infinite cylinder.

5 Conclusion

The results were within the expected values and they revealed to have a resonable physical behavior for the SRM thermal problem. For the future, it is needed a inverse problem test to be conducted in order for RTA to be validated. While this does not occur, RTA is presented here with promising results and a image of the final user interface of the sofware can be seen below.

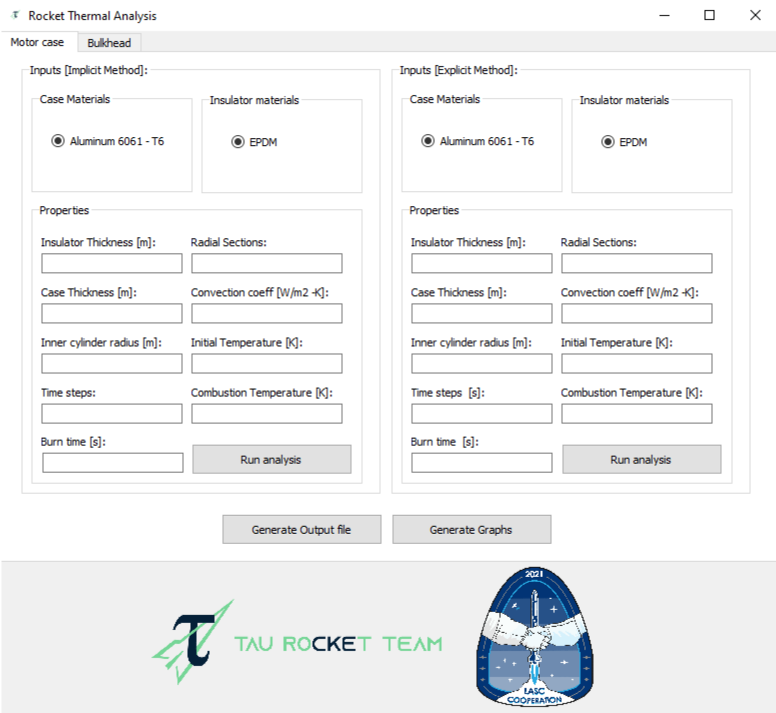

Figure 10: Main graphical user interface of RTA

References

[1] T. L. B. A. S. L. Frank P. Incropera, David P. DeWitt. *Fundamentals of Heat and Mass Transfer*. John Wiley & Sons, 6^{th} edition, 2006.

[2] O. B. George Paul Sutton. *Rocket Propulsion Elements*. John Wiley & Sons, 9^{th} edition, 2010.

[3] D. M. K. W. Morton. *Numerical Solution of Partial Differential Equations*. Cambridge University Press, 2^{nd} edition, 2005.

[4] R. Nakka. Richard nakka's experimental rocketry web site, October 19, 2020. Access in 24 october, 2020. URL: http://www.nakka-rocketry.net/.

Annex I - Casing Model

Analytical Equations

1-D Cylindrical Heat Cunduction Equation

$$\frac{1}{\alpha}\frac{\partial T}{\partial t} = \frac{\partial^2 T}{\partial r^2} + \frac{1}{r}\frac{\partial T}{\partial r}$$

1-D Conservation of Energy Equation with Convection

$$\rho c_p \frac{\partial T}{\partial t} = k \left.\frac{\partial T}{\partial r}\right|_{back} + h_m(T_c - T_w)$$

Newton's Law of cooling

$$q" = h_m(T_c - T_w)$$

Convective Heat Coefficent in Circular Tube with Turbulent Flow

$$h_m = 0.023\frac{k}{D}Re_D^{0.8}Pr^{0.3}$$

Discrete Equations

Implicit Discretization

First r node

$$\rho c_p \left(\frac{T_j^{i+1} - T_j^i}{\Delta t}\right) = k\left(\frac{T_{j+1}^{i+1} - T_j^{i+1}}{\Delta r}\right) + h_m(T_c - T_j^i)$$

$$\left(1 - \frac{h_m \Delta t}{\rho c_p}\right) T_j^i + \frac{h_m \Delta t T_c}{\rho c_p} = \left(1 + \frac{k\Delta t}{\rho c_p \Delta r}\right) T_j^{i+1} + \left(\frac{-k\Delta t}{\rho c_p \Delta r}\right) T_{j+1}^{i+1}$$

Inner r node

$$\frac{1}{\alpha}\frac{T_j^{i+1} - T_j^i}{\Delta t} = \frac{T_{j+1}^{i+1} + T_{j-1}^{i+1} - 2T_j^{i+1}}{(\Delta r)^2} + \frac{T_{j+1}^{i+1} - T_{j-1}^{i+1}}{2r\Delta r}$$

$$T_j^i = \left(1 + \frac{2\alpha\Delta t}{(\Delta r)^2}\right) T_j^{i+1} + \left(\frac{\alpha\Delta t}{2r\Delta r} - \frac{\alpha\Delta t}{(\Delta r)^2}\right) T_{j-1}^{i+1} + \left(\frac{-\alpha\Delta t}{2r\Delta r} - \frac{\alpha\Delta t}{(\Delta r)^2}\right) T_{j+1}^{i+1}$$

Last r node

$$\frac{1}{\alpha}\frac{T_j^{i+1}-T_j^i}{\Delta t}=\frac{T_{j+2}^{i+1}+T_j^{i+1}-2T_{j+1}^{i+1}}{(\Delta r)^2}+\frac{T_{j+1}^{i+1}-T_j^{i+1}}{r\Delta r}$$

$$T_j^i=\left(1-\frac{\alpha\Delta t}{(\Delta r)^2}+\frac{\alpha\Delta t}{r\Delta r}\right)T_j^{i+1}+\left(\frac{-\alpha\Delta t}{(\Delta r)^2}\right)T_{j+2}^{i+1}+\left(\frac{2\alpha\Delta t}{(\Delta r)^2}-\frac{\alpha\Delta t}{r\Delta r}\right)T_{j+1}^{i+1}$$

Explicit Discretization

First r node

$$\rho c_p\left(\frac{T_j^{i+1}-T_j^i}{\Delta t}\right)=k\left(\frac{T_{j+1}^i-T_j^i}{\Delta r}\right)+h(T_c-T_j^i)$$

$$T_j^{i+1}=\left(1-\frac{k\Delta t}{\rho c_p\Delta r}-\frac{h_m\Delta t}{\rho c_p}\right)T_j^i+\left(\frac{k\Delta t}{\rho c_p\Delta r}\right)T_{j+1}^i+\frac{h_mT_c\Delta t}{\rho c_p}$$

Inner r node

$$\frac{1}{\alpha}\frac{T_j^{i+1}-T_j^i}{\Delta t}=\frac{T_{j+1}^i+T_{j-1}^i-2T_j^i}{(\Delta r)^2}+\frac{T_{j+1}^i-T_{j-1}^i}{2r\Delta r}$$

$$T_j^{i+1}=\left(1-\frac{2\alpha\Delta t}{(\Delta r)^2}\right)T_j^i+\left(\frac{\alpha\Delta t}{(\Delta r)^2}-\frac{\alpha\Delta t}{2r\Delta r}\right)T_{j-1}^i+\left(\frac{\alpha\Delta t}{2r\Delta r}+\frac{\alpha\Delta t}{(\Delta r)^2}\right)T_{j+1}^i$$

Last r node

$$\frac{1}{\alpha}\frac{T_j^{i+1}-T_j^i}{\Delta t}=\frac{T_{j+2}^i+T_j^i-2T_{j+1}^i}{(\Delta r)^2}+\frac{T_{j+1}^i-T_j^i}{r\Delta r}$$

$$T_j^{i+1}=\left(1+\frac{\alpha\Delta t}{(\Delta r)^2}-\frac{\alpha\Delta t}{r\Delta r}\right)T_j^i+\left(\frac{\alpha\Delta t}{(\Delta r)^2}\right)T_{j+2}^i+\left(\frac{\alpha\Delta t}{r\Delta r}-\frac{2\alpha\Delta t}{(\Delta r)^2}\right)T_{j+1}^i$$

Annex II - Bulkhead Model

Analytical Equations

2-D Cylindrical Heat Conduction Equation

$$\frac{1}{\alpha}\frac{\partial T}{\partial t} = \frac{\partial^2 T}{\partial r^2} + \frac{1}{r}\frac{\partial T}{\partial r} + \frac{\partial^2 T}{\partial z^2}$$

2-D Conservation of Energy Equation with Convection

$$\frac{\rho c_p \Delta r \Delta z}{2}\frac{\partial T}{\partial t} = \frac{k\Delta z}{2}\left.\frac{\partial T}{\partial r}\right|_{up} + \frac{k\Delta z}{2}\left.\frac{\partial T}{\partial r}\right|_{down} + \frac{k\Delta r}{2}\left.\frac{\partial T}{\partial z}\right|_{back} + h\Delta r(T_c - T_w)$$

Discrete Equations

Explicit Discretization

First z and first r node

$$\frac{\rho c_p \Delta r \Delta z}{2}\left(\frac{T_{j,l}^{i+1} - T_{j,l}^{i}}{\Delta t}\right) = \frac{k\Delta z}{2}\left(\frac{T_{j+1,l}^{i} - T_{j,l}^{i}}{\Delta r}\right) + \frac{k\Delta r}{2}\left(\frac{T_{j,l+1}^{i} - T_{j,l}^{i}}{\Delta z}\right) + h_m \Delta r(T_c - T_{j,l}^{i})$$

$$T_{j,l}^{i+1} = \frac{2h_m\Delta t(T_c)}{\rho c_p \Delta z} + \left(1 - \frac{k\Delta t}{\rho c_p \Delta r^2} - \frac{k\Delta t}{\rho c_p \Delta z^2} - \frac{2h_m \Delta t}{\rho c_p \Delta z}\right)T_{j,l}^{i} + \left(\frac{k\Delta t}{\rho c_p \Delta r^2}\right)T_{j+1,l}^{i} + \left(\frac{k\Delta t}{\rho c_p \Delta z^2}\right)T_{j,l+1}^{i}$$

First z and inner r node

$$\frac{\rho c_p \Delta r \Delta z}{2}\left(\frac{T_{j,l}^{i+1} - T_{j,l}^{i}}{\Delta t}\right) = \frac{k\Delta z}{2}\left(\frac{T_{j+1,l}^{i} - T_{j,l}^{i}}{\Delta r}\right) + \frac{k\Delta z}{2}\left(\frac{T_{j,l}^{i} - T_{j-1,l}^{i}}{\Delta r}\right) + \frac{k\Delta r}{2}\left(\frac{T_{j,l+1}^{i} - T_{j,l}^{i}}{\Delta z}\right) + h_m dr(T_c - T_{j,l}^{i})$$

$$T_{j,l}^{i+1} = \frac{2h_m\Delta t(T_c)}{\rho c_p \Delta z} + \left(1 - \frac{k\Delta t}{\rho c_p \Delta z^2} - \frac{2h_m \Delta t}{\rho c_p \Delta z}\right)T_{j,l}^{i} + \left(\frac{k\Delta t}{\rho c_p \Delta r^2}\right)T_{j+1,l}^{i} + \left(\frac{-k\Delta t}{\rho c_p \Delta r^2}\right)T_{j-1,l}^{i} + \left(\frac{k\Delta t}{\rho c_p \Delta z^2}\right)T_{j,l+1}^{i}$$

First z and last r node

$$\frac{\rho c_p \Delta r \Delta z}{2}\left(\frac{T_{j,l}^{i+1}-T_{j,l}^{i}}{\Delta t}\right)=\frac{k\Delta z}{2}\left(\frac{T_{j,l}^{i}-T_{j-1,l}^{i}}{\Delta r}\right)+\frac{k\Delta r}{2}\left(\frac{T_{j,l+1}^{i}-T_{j,l}^{i}}{\Delta z}\right)+h_m\Delta r(T_c-T_{j,l}^{i})$$

$$T_{j,l}^{i+1}=\frac{2h_m\Delta t(T_c)}{\rho c_p\Delta z}+\left(1+\frac{k\Delta t}{\rho c_p\Delta r^2}-\frac{k\Delta t}{\rho c_p\Delta z^2}-\frac{2h_m\Delta t}{\rho c_p\Delta z}\right)T_{j,l}^{i}+\left(\frac{-k\Delta t}{\rho c_p\Delta r^2}\right)T_{j-1,l}^{i}$$

$$\left(\frac{k\Delta t}{\rho c_p\Delta z^2}\right)T_{j,l+1}^{i}$$

Inner z and first r node

$$\frac{1}{\alpha}\frac{T_{j,l}^{i+1}-T_{j,l}^{i}}{\Delta t}=\frac{T_{j+2,l}^{i}+T_{j,l}^{i}-2T_{j+1,l}^{i}}{(\Delta r)^2}+\frac{T_{j+1,l}^{i}-T_{j,l}^{i}}{r\Delta r}+\frac{T_{j,l+1}^{i}+T_{j,l-1}^{i}-2T_{j,l}^{i}}{(\Delta z)^2}$$

$$T_{j,l}^{i+1}=\left(1-\frac{\alpha\Delta t}{r\Delta r}+\frac{\alpha\Delta t}{(\Delta r)^2}-\frac{2\alpha\Delta t}{(\Delta z)^2}\right)T_{j,l}^{i}+\left(\frac{\alpha\Delta t}{r\Delta r}-\frac{2\alpha\Delta t}{(\Delta r)^2}\right)T_{j+1,l}^{i}+\left(\frac{\alpha\Delta t}{(\Delta r)^2}\right)T_{j+2,l}^{i}+$$

$$\left(\frac{\alpha\Delta t}{(\Delta z)^2}\right)T_{j,l-1}^{i}+\left(\frac{\alpha\Delta t}{(\Delta z)^2}\right)T_{j,l+1}^{i}$$

Inner z and inner r node

$$\frac{1}{\alpha}\frac{T_{j,l}^{i+1}-T_{j,l}^{i}}{\Delta t}=\frac{T_{j+1,l}^{i}+T_{j-1,l}^{i}-2T_{j,l}^{i}}{(\Delta r)^2}+\frac{T_{j+1,l}^{i}-T_{j-1,l}^{i}}{2r\Delta r}+\frac{T_{j,l+1}^{i}+T_{j,l-1}^{i}-2T_{j,l}^{i}}{(\Delta z)^2}$$

$$T_{j,l}^{i+1}=\left(1-\frac{2\alpha\Delta t}{(\Delta r)^2}-\frac{2\alpha\Delta t}{(\Delta z)^2}\right)T_{j,l}^{i}+\left(\frac{\alpha\Delta t}{(\Delta r)^2}-\frac{\alpha\Delta t}{2r\Delta r}\right)T_{j-1,l}^{i}+\left(\frac{\alpha\Delta t}{2r\Delta r}+\frac{\alpha\Delta t}{(\Delta r)^2}\right)T_{j+1,l}^{i}+$$

$$\left(\frac{\alpha\Delta t}{(\Delta z)^2}\right)T_{j,l-1}^{i}+\left(\frac{\alpha\Delta t}{(\Delta z)^2}\right)T_{j,l+1}^{i}$$

Inner z and last r node

$$\frac{1}{\alpha}\frac{T_{j,l}^{i+1}-T_{j,l}^{i}}{\Delta t}=\frac{T_{j-2,l}^{i}+T_{j,l}^{i}-2T_{j-1,l}^{i}}{(\Delta r)^2}+\frac{T_{j,l}^{i}-T_{j-1,l}^{i}}{r\Delta r}+\frac{T_{j,l+1}^{i}+T_{j,l-1}^{i}-2T_{j,l}^{i}}{(\Delta z)^2}$$

$$T_{j,l}^{i+1}=\left(1+\frac{\alpha\Delta t}{r\Delta r}+\frac{\alpha\Delta t}{(\Delta r)^2}-\frac{2\alpha\Delta t}{(\Delta z)^2}\right)T_{j,l}^{i}+\left(\frac{-2\alpha\Delta t}{(\Delta r)^2}-\frac{\alpha\Delta t}{r\Delta r}\right)T_{j-1,l}^{i}+\left(\frac{\alpha\Delta t}{(\Delta r)^2}\right)T_{j-2,l}^{i}+$$
$$\left(\frac{\alpha\Delta t}{(\Delta z)^2}\right)T_{j,l-1}^{i}+\left(\frac{\alpha\Delta t}{(\Delta z)^2}\right)T_{j,l+1}^{i}$$

Final z and first r node

$$\frac{1}{\alpha}\frac{T_{j,l}^{i+1}-T_{j,l}^{i}}{\Delta t}=\frac{T_{j+2,l}^{i}+T_{j,l}^{i}-2T_{j+1,l}^{i}}{(\Delta r)^2}+\frac{T_{j+1,l}^{i}-T_{j,l}^{i}}{r\Delta r}+\frac{T_{j,l-2}^{i}+T_{j,l}^{i}-2T_{j,l-1}^{i}}{(\Delta z)^2}$$

$$T_{j,l}^{i+1}=\left(1-\frac{\alpha\Delta t}{r\Delta r}+\frac{\alpha\Delta t}{(\Delta r)^2}+\frac{\alpha\Delta t}{(\Delta z)^2}\right)T_{j,l}^{i}+\left(\frac{\alpha\Delta t}{r\Delta r}-\frac{2\alpha\Delta t}{(\Delta r)^2}\right)T_{j+1,l}^{i}+\left(\frac{\alpha\Delta t}{(\Delta r)^2}\right)T_{j+2,l}^{i}+$$
$$\left(\frac{-2\alpha\Delta t}{(\Delta z)^2}\right)T_{j,l-1}^{i}+\left(\frac{\alpha\Delta t}{(\Delta z)^2}\right)T_{j,l-2}^{i}$$

Final z and inner r node

$$\frac{1}{\alpha}\frac{T_{j,l}^{i+1}-T_{j,l}^{i}}{\Delta t}=\frac{T_{j+1,l}^{i}+T_{j-1,l}^{i}-2T_{j,l}^{i}}{(\Delta r)^2}+\frac{T_{j+1,l}^{i}-T_{j-1,l}^{i}}{2r\Delta r}+\frac{T_{j,l-2}^{i}+T_{j,l}^{i}-2T_{j,l-1}^{i}}{(\Delta z)^2}$$

$$T_{j,l}^{i+1}=\left(1-\frac{2\alpha\Delta t}{(\Delta r)^2}+\frac{\alpha\Delta t}{(\Delta z)^2}\right)T_{j,l}^{i}+\left(\frac{\alpha\Delta t}{(\Delta r)^2}-\frac{\alpha\Delta t}{2r\Delta r}\right)T_{j-1,l}^{i}+\left(\frac{\alpha\Delta t}{2r\Delta r}+\frac{\alpha\Delta t}{(\Delta r)^2}\right)T_{j+1,l}^{i}+$$
$$\left(\frac{-2\alpha\Delta t}{(\Delta z)^2}\right)T_{j,l-1}^{i}+\left(\frac{\alpha\Delta t}{(\Delta z)^2}\right)T_{j,l-2}^{i}$$

Final z and last r node

$$\frac{1}{\alpha}\frac{T_{j,l}^{i+1}-T_{j,l}^{i}}{\Delta t}=\frac{T_{j-2,l}^{i}+T_{j,l}^{i}-2T_{j-1,l}^{i}}{(\Delta r)^2}+\frac{T_{j,l}^{i}-T_{j-1,l}^{i}}{r\Delta r}+\frac{T_{j,l-2}^{i}+T_{j,l}^{i}-2T_{j,l-1}^{i}}{(\Delta z)^2}$$

$$T_{j,l}^{i+1}=\left(1+\frac{\alpha\Delta t}{r\Delta r}+\frac{\alpha\Delta t}{(\Delta r)^2}+\frac{\alpha\Delta t}{(\Delta z)^2}\right)T_{j,l}^{i}+\left(\frac{-2\alpha\Delta t}{(\Delta r)^2}-\frac{\alpha\Delta t}{r\Delta r}\right)T_{j-1,l}^{i}+\left(\frac{\alpha\Delta t}{(\Delta r)^2}\right)T_{j-2,l}^{i}+$$
$$\left(\frac{-2\alpha\Delta t}{(\Delta z)^2}\right)T_{j,l-1}^{i}+\left(\frac{\alpha\Delta t}{(\Delta z)^2}\right)T_{j,l-2}^{i}$$